

# Proximity Effect in Gold Coated $\text{YBa}_2\text{Cu}_3\text{O}_7$ Films Studied by Scanning Tunneling Spectroscopy

Amos Sharoni,<sup>1</sup> Itay Aulin,<sup>1</sup> Gad Koren,<sup>2</sup> and Oded Millo<sup>1</sup>

<sup>1</sup>Racah Institute of Physics, The Hebrew University, Jerusalem 91904, Israel

<sup>2</sup>Department of Physics, Technion – Israel Institute of Technology, Haifa 32000, Israel

Scanning tunneling spectroscopy on gold layers over-coating c-axis  $\text{YBa}_2\text{Cu}_3\text{O}_7$  (YBCO) films reveals proximity induced gap structures. The gap size reduced exponentially with distance from a-axis facets, indicating that the proximity effect is primarily due to the (100) YBCO facets. The penetration depth of superconductivity into the gold is  $\sim 30$  nm, in good agreement with estimations for the dirty limit. The extrapolated gap at the interface is  $\sim 15$  meV, consistent with recent point-contact experiments. The proximity-induced order parameter appears to have predominant s-wave symmetry.

PACS numbers: 74.81.-g, 74.72.Bk, 74.50.+r

The mutual influence of a superconductor (S) in good electrical contact with a normal metal (N), a phenomenon known as the proximity effect (PE), has been studied extensively for conventional low-temperature superconductors.<sup>1,2</sup> However, the picture of the PE is not as clear for the high-temperature d-wave superconductors, such as  $\text{YBa}_2\text{Cu}_3\text{O}_7$  (YBCO), both experimentally and theoretically. In particular, local probe measurements of the PE, such as those performed for conventional proximity systems,<sup>3,4</sup> are still lacking for these systems. In addition to the fundamental interest, the issue of the proximity effect is significant also from the point of view of applications, e.g., for superconductive electronic devices based on the Josephson effect.

In a homogeneous conventional (s-wave) superconductor, the gap in the density of states (DOS) corresponds to the superconducting pair-potential (PP), a measure of the ability of quasi-particles to form Cooper pairs.<sup>5</sup> In an N-S proximity structure, where the PP is not spatially uniform, the gap in the DOS does not necessarily reflect the PP. Ideally, an abrupt change in the pair potential can take place at the N-S interface: from a finite PP on the S side, to zero on the N side. However, the gap in the DOS, which is a measure of the local pair amplitude, may change smoothly across the interface, from the full bulk value deep in the S side to zero at a distance characterized by the penetration depth into N.<sup>1,3,4,6,7</sup>

For an anisotropic d-wave superconductor, the crystallographic orientation of the superconductor surface at the N-S interface can modify significantly the PE. For example, Josephson coupling was observed in high temperature S-N-S junctions when the normal to the junction plane was along the a-axis (transport into the a-b plane), but not when it was along the c-axis (transport perpendicular to the a-b plane).<sup>8,9</sup> This implies that Cooper pairs can leak into N only along the  $\text{CuO}_2$  planes. The penetration depth (the normal coherence length),  $\xi_n$ , of the Cooper pairs into N was extracted from the temperature and N-thickness dependencies of the critical current.<sup>9,10,11</sup> However, a direct local probe measurement showing the way in which the pair amplitude de-

cays in N has not yet been performed. Another unresolved issue is the symmetry of the proximity-induced order parameter in N, when S has a bulk d-wave PP symmetry. Theoretical calculations show that the order parameter induced in the N side can have an s-wave symmetry.<sup>12,13</sup> Kohen et al. found a  $d_{x^2-y^2}$  is PP at Au-YBCO point contact junctions, where the s component showed a systematic enhancement with increased junction transparency,<sup>14</sup> reaching a value of around 16 meV. This behavior was attributed to an unusual proximity effect that modifies the PP in YBCO near the N-S interface. In particular, it induces an s-wave component accompanied by a reduction in the dominant  $d_{x^2-y^2}$ -wave PP. A question arises now regarding the connection between this s-wave component and the proximity-induced order parameter at the N side of the interface.

The PE can be directly investigated by measuring the evolution of the proximity-induced gap in the normal metal DOS as function of the distance from the N-S interface, using scanning tunneling microscopy (STM).<sup>3,4</sup> The magnitude of this gap is a measure of the local proximity-induced pair amplitude. In this work, we used c-axis YBCO films covered with gold layers of different thickness to study this gap evolution, in correlation with the gold thickness and the local surface morphology. (Unfortunately, this geometry does not allow monitoring the PE properties at the S side, as previously done by Levi et al. for  $\text{Cu-NbTi}$  junctions.<sup>3</sup>) In the present study, the tunneling spectra revealed an exponential decay of the proximity gap with distance from a-axis facets. This indicates that the PE is primarily due to the interface between the normal metal and the (100) YBCO surface, and not with the (001) surface. Interestingly, while this facet-selectivity reflects the in-plane versus out-of-plane anisotropy in YBCO, the tunneling spectra measured on the Au layer exhibited isotropic behavior, suggesting an s-wave proximity-induced order parameter. The superconductor penetration depth into the gold film was found to be  $\xi_n \sim 30$  nm, in good agreement with theoretical estimations for the dirty limit, and the extrapolated gap at the interface was about 15 meV, in accordance with the

above observation of Kohen et al.<sup>14</sup>

Optimally doped epitaxial YBCO films of 50 nm thickness were grown on (100) SrTiO<sub>3</sub> wafers by laser ablation deposition, with c-axis orientation normal to the substrate, as described elsewhere.<sup>15</sup> Next, a gold layer was deposited in-situ by laser ablation at a temperature of 150 °C at a rate of 1 Å/s, and annealed for 1 hour at this temperature before cooling down to room temperature. A total of 12 samples were prepared with gold thickness varying between 1.5 nm to 60 nm. A bare reference YBCO film showed a sharp (0.5 K wide) transition at 90 K and gap values of 18 to 20 meV. The samples were transferred from the growth chamber in a dry atmosphere, and introduced into our cryogenic STM after being exposed to ambient air for less than 15 minutes. The YBCO films consisted of nearly square-shaped crystallites, 50-100 nm lateral size and 10-15 nm height,<sup>15,16</sup> which had relatively large (100) facets. This crystalline structure was clearly observed, yet somewhat smeared even after deposition of the thickest Au layer. The gold

films revealed a granular morphology with surface grains of 10 nm in lateral size and rms height roughness of up to 1.5 nm (see Fig.1).

Tunneling spectra ( $dI/dV$  vs.  $V$  characteristics) were obtained by numerical differentiation of  $I$ - $V$  curves that were measured in correlation with the topography by momentarily disconnecting the feedback loop. About 10 curves were acquired at each position to assure data reproducibility. We also checked the dependence of the tunneling spectra on the voltage and current settings (i.e. the tip-sample distance, or the tunneling resistance values – in the range of 100 MΩ to 1 GΩ) and found that does not affect the measured gap features. This rules out the possibility that these gaps are even partially related to single electron charging effects.<sup>17</sup>

A correlated topography/spectroscopy measurement manifesting the evolution of the gap structure with the distance from the crystallite a-axis facet is presented in

figure 2. The topographic image in Fig 2 (a) is of a 5 nm thick Au layer coating an YBCO film, showing a crystallite of about 90 nm in size (marked by a white dashed line at the lower right region). Tunneling spectra were obtained sequentially along the line marked by the arrow, and are presented in Fig 2 (b). It is evident that the gap size reduces with increased distance from the crystallite edge, and at the same time the zero bias conductance increases. As discussed in details in Ref. 15, such edges typically expose the (100) YBCO surface. Note that the maximal observed gap, just at the edge – 6.7 meV, is still much smaller than the 20 meV gap of the bare YBCO sample. This is consistent with the presence of the Au layer that determines a minimal distance from the N-S interface, corresponding to the Au film thickness (see Fig.1 (b)). At larger distances from the edge, even for thinner gold layers, the gap structure practically vanished (due to the increase of the zero bias conductance it was hard to detect gap values much smaller than 2 meV).

The results described above clearly indicate that the

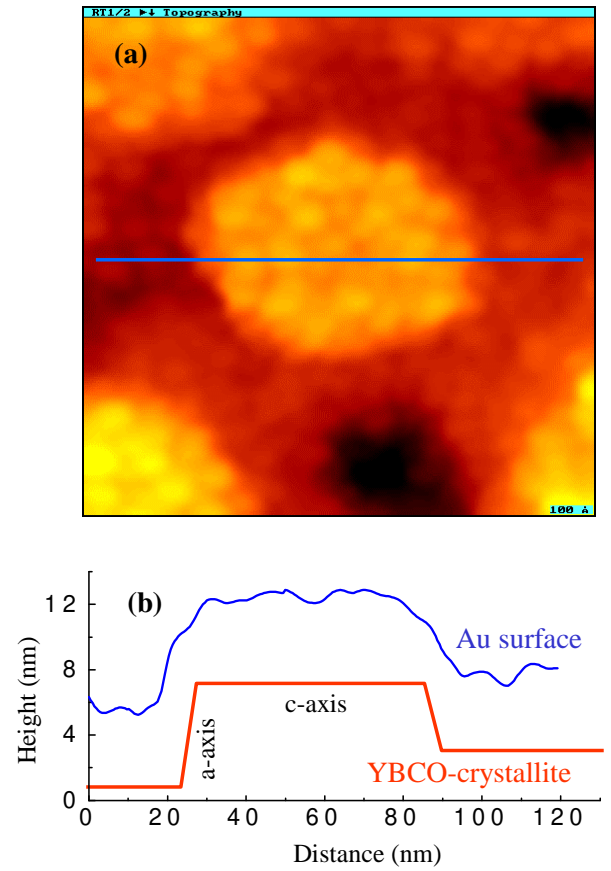


FIG. 1: (a) Topographic STM image (100 × 100 nm<sup>2</sup>) of an YBCO film coated by a 5 nm thick Au layer, showing an YBCO crystallite with clear facets and the granular morphology of the Au film. (b) A cross-section measured along the line drawn in (a) is shown together with a schematic cross-section of the underlying YBCO crystallite, with labeled facets.

PE originates primarily at the a-axis YBCO surface, whereas the contribution of the c-axis surface is negligible, in agreement with previous studies of the Josephson effect in related systems.<sup>8</sup> This behavior reflects the quasi two-dimensional d-wave symmetry of the order parameter in YBCO. However, no indication of d-wave symmetry was found for the proximity-induced pair-amplitude in gold. Unlike our previous observations for YBCO films,<sup>15</sup> the measured tunneling spectra did not exhibit anisotropy when measured on different faces of a gold grain. In particular, zero bias conductance peaks, which appear in tunneling spectra measured on the (110) surface of pure YBCO, have never been observed on gold proximity layers thicker than 7 nm (on the verge of full gold coverage). They were observed only rarely for the thinnest layers that we measured, 5 nm thick and less. It should be pointed out, however, that (110) facets in the underlying YBCO films were not abundant in our samples. We therefore measured a (110) YBCO film over-coated by a 7 nm Au film. Here also, zero bias conductance peaks were only rarely observed, and they

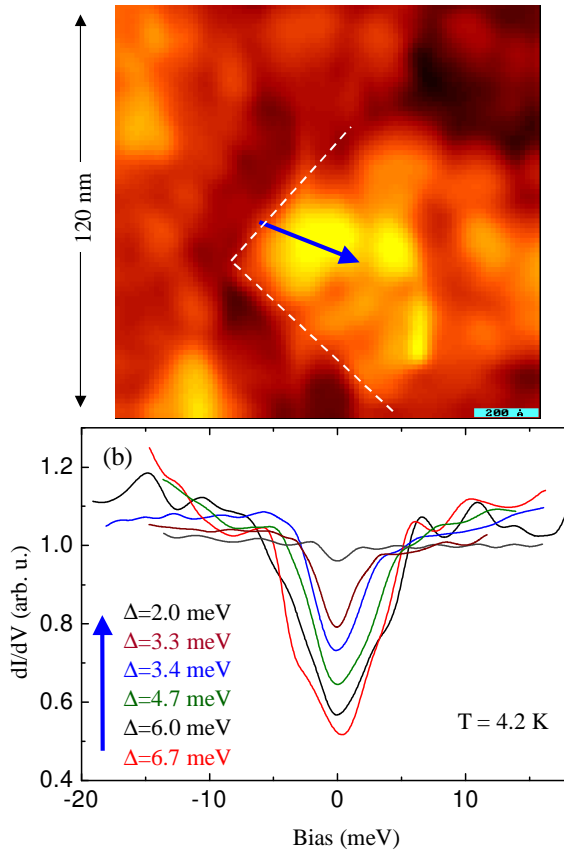


FIG. 2: A typical measurement showing the decrease in gap size as a function of the distance from a (100) facet at the crystallite edge. (a) Topographic image showing an YBCO crystallite coated with 30 nm Au. The white dashed lines show the YBCO crystallite edges, exposing (100) facets. (b) Tunneling spectra measured along the blue arrow shown. The gap sizes are denoted, from 6.7 meV (near the crystallite edge) to 2 meV (the smallest detectable gap). Note the corresponding increase of the zero bias conductance.

were much weaker as compared to those measured on the corresponding bare (110) YBCO film. The proximity induced order parameter thus appears to be predominantly s-wave in nature, as will be further discussed below.

In figure 3 we display an accumulation of the proximity gaps measured on the gold surface as a function of the distance to the closest (relevant) S-N interface (solid circles). This distance was determined from the distance to the crystallite edge, measured from the STM topographic images, taking into account the nominal thickness of the gold film (that in many cases was larger than the lateral distance to the crystallite edge). The solid line represents a best fit to the standard exponential decay form of the gap,<sup>1,6</sup>  $\Delta(x) = \Delta_0 \exp(-x/\xi_n)$ . This fit was obtained for a penetration depth (normal coherence length) of  $\xi_n \sim 29$  nm, and an interface gap value  $\Delta_0 \sim 15$  meV. Note that the value of  $\xi_n$  is much larger than the rms roughness of the gold films (less than 1.5 nm), thus local height fluctuations of the Au layer do not affect much the measured

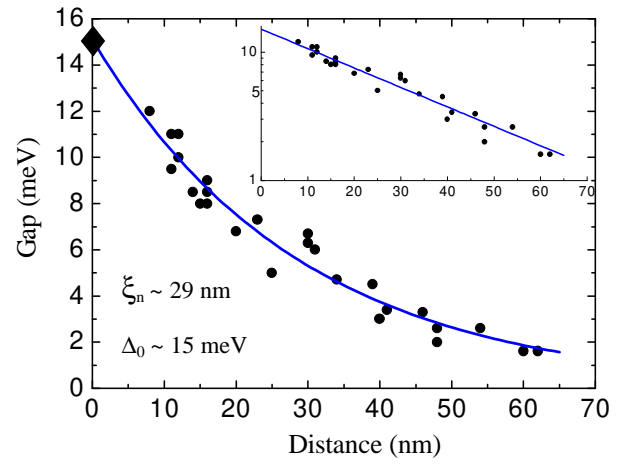


FIG. 3: Measured gap size as a function of distance from the N-S interface (solid circles). The distance is estimated from the distance to the crystallite edge, measured from the STM topographic images, taking into account the nominal Au film thickness. The solid line is a fit to a decaying exponential form, with normal coherence length (penetration depth)  $\xi_n \sim 29$  nm, and interface gap value  $\Delta_0 \sim 15$  meV (the diamond symbol). The inset shows the data in a semi-log scale.

gaps.

The value extracted for the penetration depth is very close to that estimated for the dirty limit,<sup>1</sup>  $\xi_N = (\frac{\hbar V_{FN} l_N}{6 k_B T}) \sim 33$  nm. The latter estimation was obtained assuming that the elastic mean free path  $l_N$  in the gold film is governed by grain boundary scattering, thus  $l_N \sim 10$  nm, and taking the Fermi velocity in gold from the literature,  $V_{FN} = 1.4 \times 10^6$  m/s.

More interesting is the value we found for  $\Delta_0$ . This value is similar to the magnitude of the s-wave order parameter component observed in YBCO in the point-contact experiments of Kohen et al.,<sup>14</sup> for the most transparent Au-YBCO junctions measured. This s-wave component induced near the surface of YBCO, which has a dominant  $d_{x^2-y^2}$ -wave order parameter, was attributed to an anomalous N-S proximity effect. We expect that in our samples, the Au-YBCO electrical contact (or junction transparency) is at least as good as in the most transparent junctions reported in Ref. 14 since our Au films were deposited onto the YBCO surface in-situ, without breaking the vacuum. Therefore, a strong s-wave component is probably induced in our case, and it is possible that it is this component, and not the dominant  $d_{x^2-y^2}$  order parameter, which takes part in inducing the pair amplitude at the N side of the Au-YBCO junctions.

In summary, tunneling spectroscopy correlated with topographic measurements was used to observe the proximity effect on the normal side of highly transparent YBCO-Au junctions. The proximity-induced gap in Au decays exponentially with distance from a-axis YBCO facets, indicating that the PE is primarily due to the (100) YBCO surface. Interestingly, while this facet-selectivity reflects the anisotropic nature of superconduc-

tivity in YBCO, the proximity-induced superconductivity appeared to be isotropic, s-wave in nature. In particular, the interface gap correlates well with the recently observed proximity-induced s-wave order parameter in YBCO,<sup>14</sup> and the coherence length in Au,  $\xi_n \approx 30$  nm, conforms to 'conventional' PE in the dirty limit.

relevant length scale in our experiment is the distance from an a-axis facet and not the Au thickness, and Amir Kohen for helpful discussions. The research was supported in parts by the Israel Science Foundation and the Heinrich Hertz Minerva center for high-temperature superconductivity.

#### Acknowledgments

We thank Guy Deutscher for suggesting that the most

---

Electronic address: milode@vm.shu.jil.ac.il

- <sup>1</sup> G. Deutscher and P. G. De Gennes, *Superconductivity* (Marcel Dekker, Inc., New York, 1969).
- <sup>2</sup> E. L. Wolf, *Principles of Electron Tunneling Spectroscopy* (Oxford University Press, New York, 1985).
- <sup>3</sup> Y. Levi, O. Millo, N. D. Rizzo, D. E. Prober and L. R. Motowidlo, *Phys. Rev. B* **58**, 15128 (1998).
- <sup>4</sup> N. Moussey, H. Courtois, and B. Pannetier, *Europhys. Lett.* **55**, 861 (2001).
- <sup>5</sup> P. G. de Gennes, *Superconductivity of Metals and Alloys* (Benjamin, New York, 1966).
- <sup>6</sup> W. Belzig, C. Bruder, and G. Schon, *Phys. Rev. B* **54**, 9443 (1996).
- <sup>7</sup> S. Gueron, H. Pothier, N. O. Birge, D. Esteve and M. H. Devoret, *Phys. Rev. Lett.* **77**, 3025 (1996).
- <sup>8</sup> M. A. M. Gijb, D. Scholten, Th. van Rooy and A. M. Gerrits, *Appl. Phys. Lett.* **57**, 2600 (1990).

- <sup>9</sup> H. Z. Durusoy, D. Lew, L. Lombardo, A. Kapitulnik, T. H. Geballe and M. R. Beasley, *Physica C* **266**, 253 (1996).
- <sup>10</sup> E. Polturak, G. Koren, D. Cohen, E. Aharoni and G. Deutscher, *Phys. Rev. Lett.* **67**, 3038 (1991).
- <sup>11</sup> J. Gao, W. A. M. Aamink, G. J. Gerritsma and H. Rogalla, *Physica C* **171**, 126 (1990).
- <sup>12</sup> Y. Ohashi, *J. Phys. Soc. Jpn.* **65**, 823 (1996).
- <sup>13</sup> A. A. Golubov and M. Y. Kpriyanov, *JETP Lett.* **67**, 501 (1998).
- <sup>14</sup> A. Kohen, G. Leibovitch and G. Deutscher, *Phys. Rev. Lett.* **90**, 207005 (2003).
- <sup>15</sup> A. Sharoni, G. Koren and O. Millo, *Europhys. Lett.* **54**, 675 (2001).
- <sup>16</sup> O. Neshet, G. Koren, E. Polturak and G. Deutscher, *Appl. Phys. Lett.* **72**, 1769 (1996).
- <sup>17</sup> E. Bar-Sadeh and O. Millo, *Phys. Rev. B* **53**, 3482 (1996).